

Neat1 decreases neuronal apoptosis after oxygen and glucose deprivation

<https://doi.org/10.4103/1673-5374.314313>

Date of submission: October 8, 2020

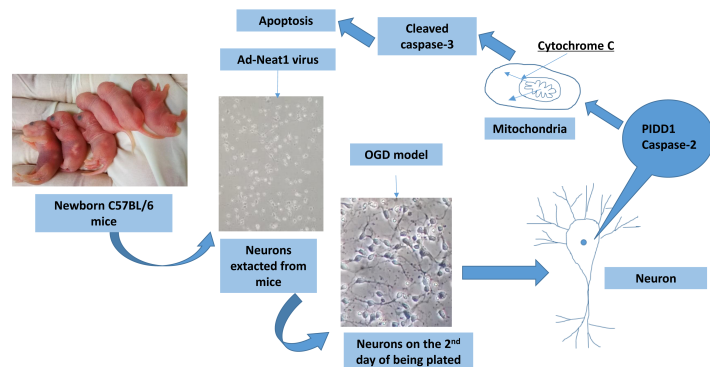
Date of decision: October 18, 2020

Date of acceptance: December 3, 2020

Date of web publication: June 7, 2021

Wei-Na Chai, Yi-Fan Wu, Zhi-Min Wu, Yan-Feng Xie, Quan-Hong Shi, Wei Dan, Yan Zhan, Jian-Jun Zhong, Wei Tang, Xiao-Chuan Sun*, Li Jiang*

Graphical Abstract *Neat1 decreases neuronal apoptosis after oxygen and glucose deprivation (OGD) by influencing PIDD1-caspase-2 pathway*



Abstract

Studies have shown that downregulation of nuclear-enriched autosomal transcript 1 (Neat1) may adversely affect the recovery of nerve function and the increased loss of hippocampal neurons in mice. Whether Neat1 has protective or inhibitory effects on neuronal cell apoptosis after secondary brain injury remains unclear. Therefore, the effects of Neat1 on neuronal apoptosis were observed. C57BL/6 primary neurons were obtained from the cortices of newborn mice and cultured *in vitro*, and an oxygen and glucose deprivation cell model was established to simulate the secondary brain injury that occurs after traumatic brain injury *in vitro*. The level of *Neat1* expression in neuronal cells was regulated by constructing a recombinant adenovirus to infect neurons, and the effects of *Neat1* expression on neuronal apoptosis after oxygen and glucose deprivation were observed. The experiment was divided into four groups: the control group, without any treatment, received normal culture; the oxygen and glucose deprivation group were subjected to the oxygen and glucose deprivation model protocol; the Neat1 overexpression and Neat1 downregulation groups were treated with Neat1 expression intervention techniques and were subjected to the in oxygen and glucose deprivation protocol. The protein expression levels of neurons p53-induced death domain protein 1 (PIDD1, a pro-apoptotic protein), caspase-2 (an apoptotic priming protein), cytochrome C (a pro-apoptotic protein), and cleaved caspase-3 (an apoptotic executive protein) were measured in each group using the western blot assay. To observe changes in the intracellular distribution of cytochrome C, the expression levels of cytochrome C in the cytoplasm and mitochondria of neurons from each group were detected by western blot assay. Differences in the cell viability and apoptosis rate between groups were detected by cell-counting kit 8 assay and terminal deoxynucleotidyl transferase dUTP nick-end labeling assay, respectively. The results showed that the apoptosis rate, PIDD1, caspase-2, and cleaved caspase-3 expression levels significantly decreased, and cell viability significantly improved in the Neat1 overexpression group compared with the oxygen and glucose deprivation group; however, Neat1 downregulation reversed these changes. Compared with the Neat1 downregulation group, the cytosolic cytochrome C level in the Neat1 overexpression group significantly decreased, and the mitochondrial cytochrome C level significantly increased. These data indicate that Neat1 upregulation can reduce the release of cytochrome C from the mitochondria to the cytoplasm by inhibiting the PIDD1-caspase-2 pathway, reducing the activation of caspase-3, and preventing neuronal apoptosis after oxygen and glucose deprivation, which might reduce secondary brain injury after traumatic brain injury. All experiments were approved by the Animal Ethics Committee of the First Affiliated Hospital of Chongqing Medical University, China, on December 19, 2020 (approval No. 2020-895).

Key Words: apoptosis; caspase-2; caspase-3; cytochrome C; lncRNA-Neat1; mitochondria; neuron; OGD; PIDD1; traumatic brain injury

Chinese Library Classification No. R459.9; R363; R364

Introduction

Secondary injury following traumatic brain injury (TBI) involves a series of complicated events, resulting in neuronal apoptosis that has crucial impacts on TBI prognosis (Tang et al., 2020; Wang et al., 2020). Long noncoding RNAs (lncRNAs) are a class of RNAs that are longer than 200 nucleotides and are widely

expressed in various human tissues (Mercer et al., 2009; Reng et al., 2020; Di et al., 2021). Although lncRNAs do not encode proteins, they have been shown to play important roles at various levels of diverse cellular events, such as chromatin remodeling, epigenetic regulation, transcriptional regulation, and post-transcriptional processing (Batista and Chang, 2013;

Department of Neurosurgery, First Affiliated Hospital of Chongqing Medical University, Chongqing, China

*Correspondence to: Li Jiang, PhD, drjiangli2019@163.com; Xiao-Chuan Sun, PhD, sunxiaochuan@cqmu.edu.cn.

<https://orcid.org/0000-0002-2407-3672> (Li Jiang); <https://orcid.org/0000-0001-6992-332X> (Xiao-Chuan Sun)

Funding: This work was supported by the Youth Science Foundation Project of the National Natural Science Foundation of China, No. 81701226 (to LJ).

How to cite this article: Chai WN, Wu YF, Wu ZM, Xie YF, Shi QH, Dan W, Zhan Y, Zhong JJ, Tang W, Sun XC, Jiang L (2022) *Neat1 decreases neuronal apoptosis after oxygen and glucose deprivation. Neural Regen Res* 17(1):163-169.

Research Article

Bali and Kuner, 2014). Accumulating evidence suggests that lncRNAs are highly expressed in the central nervous system, associated with brain development and function. Previously, we showed that the expression levels of many lncRNAs in the mouse cerebral cortex surrounding the injury site change significantly after TBI, including the lncRNA nuclear-enriched autosomal transcript 1 (Neat1), which was significantly increased after TBI. Neat1 is a highly regulated, 4 kb lncRNA, is an essential architectural component of paraspeckles and has been reported to be associated with the cell death pathway, neuronal viability, and glioma cell proliferation (Guru et al., 1997; Gong et al., 2016; Zhen et al., 2016; Sunwoo et al., 2017; Zhang et al., 2020). We also demonstrated that Neat1 might be associated with PIDD1 (Zhong et al., 2017) and inhibit apoptosis and inflammation after TBI. However, the pathway through which Neat1 influences neuronal apoptosis remains unclear. A previous study showed that PIDD1 might activate caspase-2, which regulates cell death by initiating cytochrome C release from the mitochondria (Janssens and Tinel, 2012).

In the present study, the oxygen and glucose deprivation (OGD) model was generated in primary neurons to simulate secondary injury following TBI, and the mechanism through which Neat1 and PIDD1 influence neuronal apoptosis was investigated. Changes in PIDD1, caspase-2, and cytochrome C expression were examined in response to the up- and downregulation of Neat1 expression.

Materials and Methods

Animals

C57BL/6 newborn mice, weighing 1.0–1.5 g, were obtained within 24 hours of birth, regardless of sex, from the Experimental Animal Center of Chongqing Medical University, China (license No. SYXK (Yu) 2018-0003). The brains of the mice were harvested using a standard enzyme treatment protocol for neonatal mice born within the previous 24 hours (Jiang et al., 2015). The cerebral cortex was minced into 2-mm³ pieces and dissociated with 2 mg/mL papain and DNase I (Deoxyribonuclease I) (D8070, Solaribo, Beijing, China) to obtain a cell suspension. After centrifugation at 800 rpm for 8 minutes at room temperature, the resulting cell pellets were resuspended in Dulbecco's modified Eagle medium (DMEM)/F12 (#SH30023.01, Hyclone, Logan, UT, USA) containing 10% horse serum. Primary cultures were maintained on plates in a humidified incubator with 5% CO₂ and 95% air at 37°C. The culture medium was replaced with fresh medium every 48 hours. All experiments were approved by the Animal Ethics Committee of the First Affiliated Hospital of Chongqing Medical University, China, on December 19, 2020 (approval No. 2020-895). All studies involving animals were performed in accordance with the Animal Research: Reporting *In Vivo* Experiments Guidelines (ARRIVE Guidelines) for reporting experiments involving animals.

Recombinant adenovirus

Neat1 (3190 bp, NR_003513.3)-overexpression recombinant adenoviruses (up-Ad-Neat1, 2.0 × 10¹⁰ pfu/mL) and blank control overexpression recombinant adenoviruses (up-Ad-GFP, 1.1 × 10¹¹ pfu/mL), interfering recombinant adenoviruses (down-Ad-Neat1, 1.1 × 10¹¹ pfu/mL), and blank control interfering recombinant adenoviruses (down-Ad-GFP, 5 × 10¹⁰ pfu/mL) were provided by Shanghai Shenggong Biotechnology Co., Ltd. (Shanghai, China). The small interfering RNA sequence expressed by the Neat1 interfering adenovirus was as follows: 5'-CCG GGC GCT TGC TAT GAG ATC ATT GCT CGA GCA ATG ATC TCA TAG CAA GCG CTT TTT TG-3'. The virus was amplified in a human embryonic kidney cell line (containing the Ad5 E1 region) by adenovirus transduction, followed by purification (Marr et al., 1998) using classical cesium chloride gradient centrifugation. Titer detection was performed using

the Titer-EZ adenoviral titer detection kit to accelerate the titrating of adenoviruses (Bewig and Schmidt, 2000; Guo et al., 2016).

Primary neuron cultures and oxygen-glucose deprivation modeling

Primary cortical neurons were obtained from C57BL/6 newborn mice, 24 hours postnatal, as described in previous studies (Jiang et al., 2015).

The OGD model is the most common *in vitro* cell model used to study ischemic diseases. We established an OGD model to simulate TBI-induced secondary brain injury (Salvador et al., 2015) because hypoxic changes caused by cell ischemia are often accompanied by secondary brain injury. After the OGD model was established, the cell viability of neurons decreased significantly, indicating that model generation was successful. All neurons were randomly allocated to the following four groups, without blinding: the control neuron group experienced neither OGD nor Neat1 downregulation or overexpression (*n* = 3 replicates). The OGD neuron group experienced OGD and was transduced with the Ad-GFP virus (*n* = 3). The Neat1 overexpression neuron group experienced OGD and was transduced with the Ad-Neat1 overexpression virus (*n* = 3). The Neat1 downregulation neuron group experienced OGD and was transduced with the Ad-Neat1 downregulation virus (*n* = 3).

The maintenance medium was neurobasal-A (#10888022, Gibco Life Technologies, New York, USA) with 1× B27 supplement and 0.5 mM L-glutamine. The cell density on six-well plates was approximately 2.5 × 10⁶/mL. Neat1 overexpression and downregulation adenovirus were used to infect primary neurons 24 hours after plating, using multiplicities of infection of 5 and 240, respectively. Polybrene (#H9268, Sigma-Aldrich, Shanghai, China) was also added at 2 μg/mL. Neurons were photographed using a laser-scanning confocal microscope. Four groups were established as described.

The primary neurons were subjected to the OGD model as previously described (Pei et al., 2019). In brief, the neurons were washed twice with phosphate-buffered saline (PBS) and incubated in glucose-free DMEM (#2044490, Gibco Life Technologies, New York, USA) in a hypoxic chamber (1% O₂, 5% CO₂, and 94% N₂) at 37°C for 3 hours. Afterward, the neurons were incubated in normal media under normoxic conditions (5% CO₂ and 95% O₂) at 37°C for 24 hours. All cells were counted using ImageJ software (NIH, Bethesda, MD, USA).

Identification of neurons by laser-scanning confocal microscope

The neurons were inoculated on 11-mm chamber slides coated with poly-L-lysine at a concentration of 2.5 × 10⁶ cells/mL; the volume of each well was 0.5 mL (in a 24-well plate). On the fifth day of culture, neurons were identified by immunofluorescence using a primary rabbit-anti-mouse β-tubulin III antibody (1:200; Cell Signaling Technology, Danvers, MA, USA) and a secondary goat-anti-rabbit Dylight 488 antibody (1:200; Cell Signaling Technology). Cell nuclei were stained with 4',6-di-amidino-2-phenylindole (DAPI; Sigma-Aldrich). Images were captured using a laser-scanning confocal microscope (Zeiss, Jena, Germany). ImageJ software (NIH, Bethesda, MD, USA) was used to count the number of β-tubulin III-positive cells and the percentage of β-tubulin-III-positive cells to DAPI-positive cells. At least six visual fields from each slide were selected to count the number of positive cells. Staining experiments were performed at least three independent times.

Cell viability assay

These experiments were performed 24 hours after OGD exposure. The cells of the four described groups were

inoculated in 96-well plates (six wells for each group) at a concentration of 2.5×10^6 cells/mL, and cell viability was assessed after 24 hours of OGD exposure using a cell-counting kit 8 (CCK-8) assay (Beyotime Biotechnology, Nanjing, China). Prior to evaluation, the cells were washed with 0.1 mL of 10% CCK-8 base medium and then incubated for 4 hours (5% CO₂, 37°C). After incubation, the cells were measured at a wavelength of 450 nm using a spectrophotometer (ThermoFisher, New York, USA). The experiments were repeated three times on different days, and the average absorbance was obtained.

Cell apoptosis assay

These experiments were performed 24 hours after OGD exposure. The neurons were inoculated on 11-mm chamber slides coated with poly-L-lysine at a concentration of 2.5×10^6 cells/mL and 0.5 mL per well (in a 24-well plate). The control, OGD, *Neat1* overexpression, and *Neat1* downregulation groups were established as described above. Twenty-four hours after OGD, the four groups of cells were fixed with 2% paraformaldehyde for 30 minutes and washed three times with PBS for 3 minutes each time. Cells were incubated with 0.3% Triton X-100 at room temperature for 5 minutes. An appropriate amount of terminal deoxynucleotidyl transferase dUTP nick-end label (TUNEL, #C1090; Beyotime Biotechnology) detection solution was prepared, and the neurons were washed twice with PBS. The neurons were incubated with 50 μ L TUNEL solution per sample at 37°C for 60 minutes. Cell nuclei were stained with 4',6-diamidino-2-phenylindole (DAPI; Sigma-Aldrich). Following three washes with PBS, coverslips were mounted onto the slides using an anti-fade mounting medium (Beyotime Biotechnology). Afterward, the apoptotic nuclei in neurons were observed by laser-scanning confocal microscopy. Six images were randomly selected in each group, and the numbers of TUNEL-positive cells and DAPI-positive cells were counted with ImageJ software (NIH, Bethesda, MD, USA). The results are reported as the percentage of TUNEL-positive cells relative to DAPI-positive cells. The experiment was repeated three independent times.

Reverse-transcription polymerase chain reaction

The experiments were performed after 2, 3, 4, 5, or 6 hours of OGD exposure. Neurons for reverse-transcription-polymerase chain reaction (RT-PCR) were inoculated in six-well plates at a concentration of 2.5×10^6 cells/mL at 1 mL per well. The primer sequences used for *Neat1* and β -*actin* detection are shown in **Table 1**. Genomic DNA was removed by treatment with 2 μ L 5% gDNA Eraser Buffer, 1 μ L gDNA Eraser, combined with 1 μ g total RNA extracted by using TRIzol reagent (ThermoFisher, New York, USA), and RNase-free dH₂O to 10 μ L and reacted at 42°C for 2 minutes. A reaction solution containing Prime Script RT Enzyme Mix I (1 μ L), RT Primer Mix (4 μ L), 5% Prime Script Buffer 2 (4 μ L), and RNase-free dH₂O (1 μ L) was combined and incubated for 15 minutes at 37°C, followed by 85°C for 5 seconds. RT-PCR used the following system: 10 μ L TB Green Premix Ex Taq II (2 \times Tli RNaseH Plus), 0.8 μ L PCR Forward Primer (10 μ M), 0.8 μ L PCR Reverse Primer (10 μ M), 0.4 μ L ROX Reference Dye (50 \times), 2 μ L DNA template, and 6 μ L RNase water (Code No. RR820A; Takara, Tokyo, Japan). The PCR was performed at 5°C for 2 minutes, 95°C for 10 minutes, and then the relative expression was determined by 40 cycles (95°C for 15 seconds, 60°C for 60 seconds). The relative expression level was quantified using the $2^{-\Delta\Delta CT}$ method (Yang et al., 2014).

Western blot assay

These experiments were performed 24 hours after OGD. Neurons for western blot assay were inoculated in six-well plates at a concentration of 2.5×10^6 cells/mL at 1 mL per well. Whole-cell protein was extracted using radioimmunoprecipitation assay (RIPA) buffer containing

Table 1 | Primer sequences used in this study

Gene	Sequence (5'–3')	Product size (bp)
<i>Neat1</i>	Forward: GAA GCG GGG CTA AGT ATA AA	175
	Reverse: CCA TGT AGG CCT GTG AAA CT	
β - <i>Actin</i>	Forward: GTG CTA TGT TGC TCT AGA CTT CG	174
	Reverse: ATT CCA CAG GAT TCC ATA CC	

1 mM phenylmethanesulfonyl fluoride and 2% protease inhibitor cocktail (Beyotime Biotechnology). The mitochondrial proteins were extracted using a cell mitochondrial separation kit (Beyotime Biotechnology), and the mitochondria were lysed using a mitochondrial lysis solution (Beyotime Biotechnology) with 1 mM phenylmethanesulfonyl fluoride. The protein lysate was separated by 12% sodium dodecyl sulfate-polyacrylamide gel electrophoresis and transferred to a 0.45- μ m polyvinylidene fluoride membrane (Millipore Corp, Billerica, MA, USA). Monoclonal antibodies against p53-induced death domain 1 (PIDD1, 1:500; Rabbit#12119-1-AP, Sanying Biotechnology Co., Ltd., Wuhan, China), caspase-2 (1:200; Rabbit# ERP16796, ab179520, ABCAM, Cambridge, MA, USA), cleaved caspase-3 (1:500; Rabbit# GB11009,171905, Wuhan Goodbio Technology, China); cytochrome C (1:1000; Rabbit# ERP1327, ab133504, ABCAM), and β -actin (1:500; Rabbit#21338, Signalway, CA, USA) were used as primary antibodies, incubated overnight at 4°C. Horseradish peroxidase-conjugated AffiniPure anti-Rabbit IgG (1:4000; Goat#SA00001-2, Sanying Biotechnology Co.) was used as the secondary antibody, incubated for 1 hour at 37°C. Proteins in the membranes were visualized using an enhanced chemiluminescence reagent (Millipore) and a Fusion Solo 6S image analysis system (Vilber Lourmat, Paris, France). Relative protein optical intensities (ratio of the target protein to internal loading control) were quantified using Gel-Pro Analyzer 4.0 software (Media Cybernetics, Silver Spring, MD, USA).

Statistical analysis

All data are presented as the mean \pm standard deviation (SD) and were analyzed with Graphpad Prism 8.0 software (GraphPad Software, San Diego, CA, USA). The data for relative gene expression, apoptosis rate, relative protein expression, and cell viability were analyzed using one-way analysis of variance followed by Tukey's *post hoc* test. $P < 0.05$ was considered significant.

Results

Primary neuronal culture

Morphological observations of primary cortical neurons showed that the neuronal bodies were fusiform under a light microscope, and the nerve cells featured multiple processes, which connected the nerve cells to each other, forming a neural network (**Figure 1**). Using fluorescence microscopy, the neuronal cells, especially the axons, showed corresponding green fluorescence (β -tubulin III-positive cells), which confirmed that these cells were neurons (**Figure 2**). All neurons in the visual field were counted using ImageJ software, and greater than 90% of the cells were neurons, which indicated that the purity of the cultured neurons was high.

Neat1 expression in primary mouse cortical neurons is upregulated after OGD

Total RNA was extracted from the control and OGD-exposed groups (exposed to OGD for 2, 3, 4, 5, or 6 hours on the fifth day of culture) 24 hours after OGD exposure. RT-PCR showed that *Neat1* levels increased after 2 and 3 hours of OGD in the OGD group compared with those in the control group (**Figure 3**).



Figure 1 | Neurons from the cerebral cortex of C57BL/6 mice, 2 days after plating, by light microscopy.

The neuronal bodies were fusiform, and the neurons featured multiple processes, which connected with other neurons, forming a neural network. Original magnification, 100x.

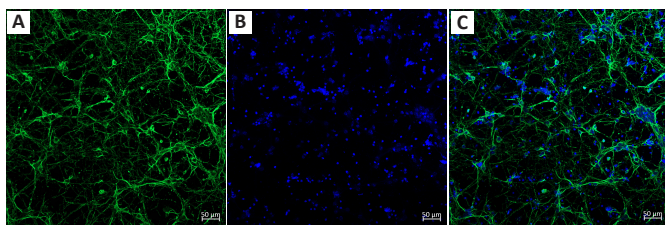


Figure 2 | Immunofluorescence identification of β -tubulin III-labeled neurons from the cerebral cortex of C57BL/6 mice, 5 days after plating (laser-scanning confocal microscope).

The cells with green fluorescence in the visual field were neurons. (A) β -Tubulin III (green) was used to stain the cytoplasm and axon of neurons. (B) DAPI (blue) was used to stain the nuclei. (C) Merge of β -tubulin III and DAPI. Scale bars: 50 μ m. DAPI: 4',6-Diamidino-2-phenylindole.

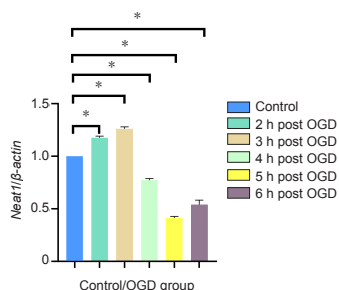


Figure 3 | Reverse transcription-polymerase chain reaction for the expression of Neat1.

Neat1 expression increased significantly in primary neurons from the cerebral cortex of C57BL/6 mice after establishing the OGD model for 2 hours. The highest level was obtained after 3 hours of OGD modeling and then gradually decreased. The Y-axis represents the ratio of relative gene expression between Neat1 and β -actin. Data are shown as the mean \pm SD, and each experiment was repeated at least in triplicate ($n = 3$, one-way analysis of variance followed by Tukey's *post hoc* test). * $P < 0.05$. Neat1: Nuclear-enriched autosomal transcript 1; OGD: oxygen and glucose deprivation.

Influence of Neat1 overexpression or downregulation on PIDD1, caspase-2, cytochrome C, and cleaved caspase-3 expression

Western blot assay results showed that the expression level of PIDD1 in the Neat1 downregulation group was significantly higher than those in the OGD, control, and Neat1 overexpression groups (Figure 4). The expression level of PIDD1 in the control group was the lowest among the four groups (Figure 4). The expression level of PIDD1 in the Neat1 overexpression group was significantly lower than those in the OGD ($P < 0.05$) and Neat1 downregulation group but significantly higher than that in the control group (Figure 4).

Similarly, the expression level of caspase-2 in the Neat1 downregulation group was highest among the four groups, significantly higher than those in the OGD ($P < 0.05$), control, and Neat1 overexpression groups. The expression level of caspase-2 was significantly lower in the control group compared with those in the other three groups. The expression level of caspase-2 in the Neat1 overexpression group was also significantly lower than those in the OGD ($P < 0.05$) and Neat1 downregulation groups but was significantly higher than that in the control group (Figure 4).

Caspase-2 can permeabilize the outer mitochondrial membrane, facilitating the release of cytochrome C from the

mitochondria to the cytoplasm, where it binds apoptosis-related factor 1 (Apaf-1), promoting the formation and activation of caspase-9-containing apoptotic bodies. Activated caspase-9 can activate the apoptosis executive protein caspase-3. Therefore, cytosolic cytochrome C was harvested and analyzed. Western blot assay results showed that the levels of cytosolic cytochrome C were significantly different among the four groups. The Neat1 downregulation group had the highest level of cytosolic cytochrome C, whereas the control group had the lowest level, compared with the other groups. The cytosolic cytochrome C level of the Neat1 overexpression group was significantly lower than that in the OGD group ($P < 0.05$) but significantly higher than that in the control group (Figure 5).

Furthermore, the levels of cleaved caspase-3 showed significant differences among the four groups. As shown by western blot assay results, the levels of cleaved caspase-3 in the Neat1 downregulation group were significantly higher than those in the OGD, control, and Neat1 overexpression groups. The level of cleaved caspase-3 was the lowest in the control group compared with those in the other three groups. The level of cleaved caspase-3 in the Neat1 overexpression group was significantly higher than that in the control group but significantly lower than that in the OGD group ($P < 0.05$; Figure 6).

In summary, the levels of PIDD1, caspase-2, cleaved caspase-3, and cytosolic cytochrome C were significantly higher in the Neat1 downregulation group but significantly lower in the control group compared with those in the other groups. The levels of PIDD1, caspase-2, cleaved caspase-3, and cytosolic cytochrome C in the Neat1 overexpression group were significantly higher than those in the control group but significantly lower than those in the OGD group.

Neat1 overexpression and downregulation affect the viability and apoptosis rate of cultured neurons *in vitro*

To study the influence of Neat1 expression in neurons, the cell viability and apoptosis rate of neurons were measured under different conditions using the CCK-8 and TUNEL assays, respectively. The optical density of the Neat1 downregulation group was significantly lower than those of the other groups, indicating that neurons in the Neat1 downregulation group had the lowest viability. The optical density of the Neat1 overexpression group was significantly higher than that of the OGD group ($P < 0.05$) but significantly lower than that of the control group, indicating that neurons in the Neat1 overexpression group had significantly increased viability compared with the OGD group ($P < 0.05$) but significantly reduced viability compared with the control group (Figure 7).

Furthermore, neurons from the different treatment groups were collected to examine the apoptosis rate by TUNEL assay. The positive rate of TUNEL staining was highest in the Neat1 downregulation group and lowest in the control group, suggesting that the Neat1 downregulation group had the highest neuron apoptosis rate among the four groups. The positive rate of TUNEL staining in the Neat1 overexpression group was significantly lower than that in the OGD group ($P < 0.05$) but significantly higher than that in the control group, indicating that neuronal apoptosis rate was significantly lower in the Neat1 overexpression group compared with that in the OGD group but significantly higher compared with that in the control group (Figure 8).

Cytochrome C in the mitochondria is related to the change in the Neat1 expression

The release of cytochrome C from the mitochondria to the cytoplasm plays a key role in apoptosis. To study changes in cytochrome C localization in neurons, cytochrome C in the mitochondria and the cytoplasm were analyzed in the four groups.

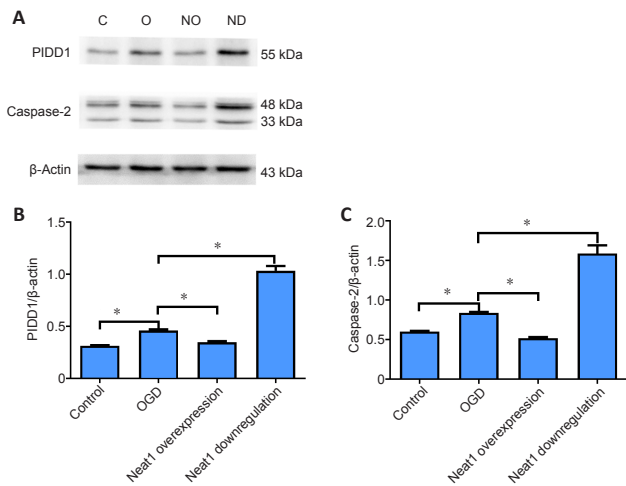


Figure 4 | Neat1 inhibits PIDD1 and caspase-2 protein expression in post-OGD neurons, 24 hours after OGD.

(A) Western blot assay of PIDD1 and caspase-2. β-Actin was used as an internal loading control. (B) Quantification of PIDD1 protein expression, normalized against β-actin expression. (C) Quantification of caspase-2 protein expression, normalized to β-actin expression. The Y-axes in B and C represent the ratios between the target protein OD and that of the loading control protein. Data are shown as the mean ± SD, and each experiment was repeated at least in triplicate ($n = 3$, one-way analysis of variance followed by Tukey's *post hoc* test). * $P < 0.05$. Neat1: Nuclear-enriched autosomal transcript 1; OD: optical density; OGD: oxygen and glucose deprivation; PIDD1: p53-induced protein with a death domain 1. C: Control group; ND: Neat1 downregulation group; NO: Neat1 overexpression group; O: OGD group.

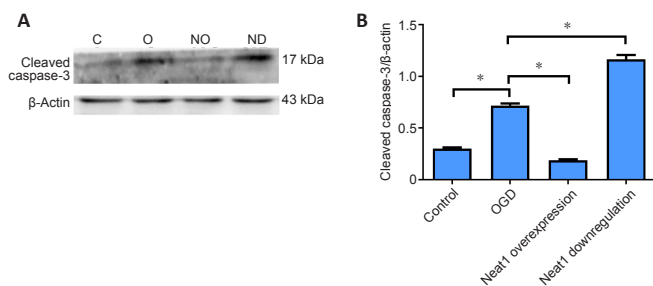


Figure 6 | Neat1 inhibits cleaved caspase-3 protein expression in post-OGD neurons 24 hours after OGD.

(A) Western blot assay of cleaved caspase-3, with β-actin as an internal loading control. (B) Quantification of cleaved caspase-3 protein expression, normalized to β-actin expression. The Y-axis of B is expressed as the ratio between the target protein OD to that of the loading control protein. Data are shown as the mean ± SD, and each experiment was repeated at least in triplicate ($n = 3$, one-way analysis of variance followed by Tukey's *post hoc* test). * $P < 0.05$. Neat1: Nuclear-enriched autosomal transcript 1; OD: optical density; OGD: oxygen and glucose deprivation. C: Control group; ND: Neat1 downregulation group; NO: Neat1 overexpression group; O: OGD group.

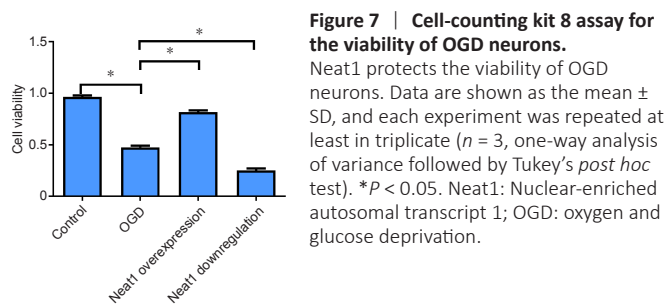


Figure 7 | Cell-counting kit 8 assay for the viability of OGD neurons.

Neat1 protects the viability of OGD neurons. Data are shown as the mean ± SD, and each experiment was repeated at least in triplicate ($n = 3$, one-way analysis of variance followed by Tukey's *post hoc* test). * $P < 0.05$. Neat1: Nuclear-enriched autosomal transcript 1; OGD: oxygen and glucose deprivation.

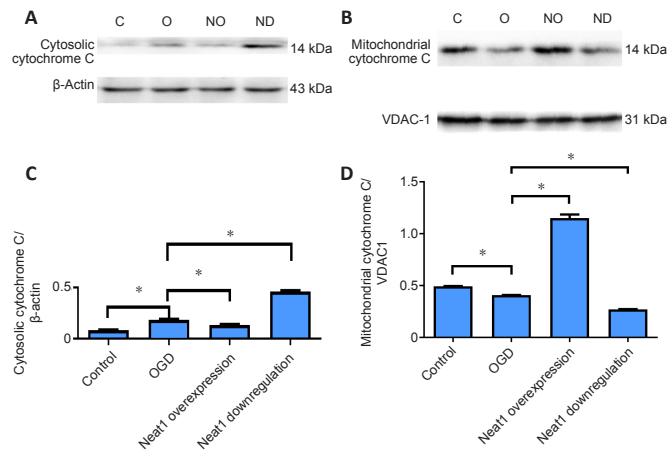


Figure 5 | Western blot assay showing the expression of cytosolic cytochrome C and mitochondrial cytochrome C.

(A) Protein levels of cytosolic cytochrome C, using β-actin as an internal loading control. (B) Protein levels of mitochondrial cytochrome C, using VDAC1 as an internal loading control. (C) Quantification of cytosolic cytochrome C protein expression, normalized to β-actin expression. (D) Quantification of mitochondrial cytochrome C protein expression, normalized to VDAC1 expression. The Y-axes represent the ratios of the target protein OD to that of the loading control protein. Data are shown as the mean ± SD, and each experiment was repeated at least in triplicate ($n = 3$, one-way analysis of variance followed by Tukey's *post hoc* test). * $P < 0.05$. Neat1: Nuclear-enriched autosomal transcript 1; OD: optical density; OGD: oxygen and glucose deprivation. C: Control group; ND: Neat1 downregulation group; NO: Neat1 overexpression group; O: OGD group; VDAC1: voltage-dependent anion channel 1.

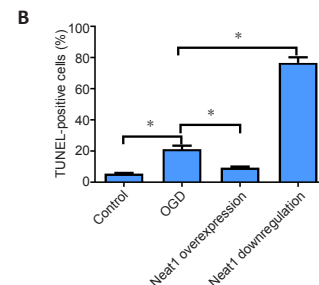
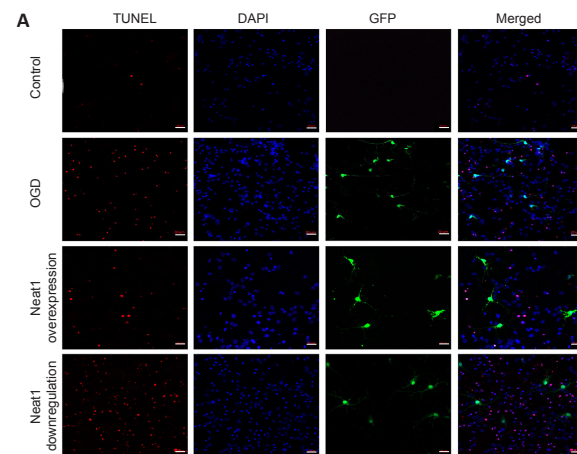


Figure 8 | TUNEL staining for neuronal apoptosis.

(A) TUNEL staining (red) and DAPI (blue) staining respectively represent apoptotic neuronal nuclei and the total cell nuclei (neurons from the cerebral cortex of C57BL/6 mice) by laser-scanning confocal microscopy (Zeiss, Jena, Germany). Green fluorescence represents GFP. Scale bars: 20 μm. (B) TUNEL-positive cells: The population of TUNEL-positive cells (red) is shown as a percentage relative to the total cell number. Data are shown as the mean ± SD, and each experiment was repeated at least in triplicate ($n = 3$, one-way analysis of variance followed by Tukey's *post hoc* test). * $P < 0.05$, vs. OGD group. DAPI: 4',6-Diamidino-2-phenylindole; GFP: green fluorescent protein; Neat1: nuclear-enriched autosomal transcript 1; OGD: oxygen and glucose deprivation; TUNEL: terminal deoxynucleotidyl transferase dUTP nick-end labeling.

Western blot assay results showed that compared with the other groups, the level of cytosolic cytochrome C was significantly higher, and the level of mitochondrial cytochrome C was significantly lower in the Neat1 downregulation group than those in all other groups; in contrast, the level of cytosolic cytochrome C was significantly lower, and the level of mitochondrial cytochrome C was significantly higher in the control group than those in the other groups. Moreover, the level of cytosolic cytochrome C was significantly lower, but the level of mitochondrial cytochrome C was significantly higher in the Neat1 overexpression group than those in the OGD group ($P < 0.05$; **Figure 8**).

Discussion

The primary purpose of this study was to explore the possible mechanism through which Neat1 affects neuronal apoptosis. As shown in our previous study (Zhong et al., 2017), the upregulation of Neat1 may reduce the apoptosis rate of neurons after a controlled cortical injury *in vivo*, but the effects of Neat1 on neurons and the potential mechanism of action are not clear. To further study the effects of Neat1 on neuronal apoptosis, primary neuronal cultures and an OGD model were established to simulate secondary injury following TBI. The OGD model is the most commonly used *in vitro* cell model to study ischemic diseases because hypoxic changes that occur during cell ischemia are often accompanied by secondary brain injury. Therefore, this study established an OGD model to simulate TBI-associated secondary brain injury (Salvador et al., 2015). The results of the present study showed that the neuronal viability was significantly reduced, and the neuronal apoptosis rate was significantly increased in the Neat1 downregulation group relative to the other treatment groups. However, in the Neat1 overexpression group, neuronal viability was significantly increased, and the neuronal apoptosis rate was significantly reduced relative to the OGD groups. This result indicated that after OGD, the upregulation of Neat1 might increase the activity of neurons reduce neuronal apoptosis, whereas the downregulation of Neat1 might result in reduced neuronal viability and increased apoptosis. Therefore, Neat1 may have a protective effect against ischemic and anoxic nerve injury, which is consistent with our previous *in vivo* study results (Zhong et al., 2017).

To deeply study the role played by Neat1 in the neuronal apoptosis pathway, the levels of several possible downstream factors were analyzed under different conditions. PIDD1 is considered to play an important role in cell apoptosis based on the findings of previous studies. PIDD1 can activate caspase-2 through the formation of a PIDD1-RAIDD-caspase-2 complex, leading to neuronal apoptosis (Janssens and Tinel, 2012; Di Donato et al., 2016). However, PIDD1 is also involved in anti-apoptotic pathways, according to some other studies; therefore, the role of PIDD1 in the apoptosis process remains under debate (Kim et al., 2009; Bock et al., 2012). In the present study, the results showed that neuronal apoptosis and the levels of PIDD1 both significantly increased in the Neat1 downregulation group but were significantly decreased in the Neat1 overexpression group, indicating that neuronal apoptosis and PIDD1 levels showed similar trends after OGD. This finding suggested that PIDD1 played a pro-apoptotic role in neuronal apoptosis after OGD, which was consistent with our previous *in vivo* study results (Zhong et al., 2017). Caspase-2, the most well-conserved member of the caspase family, is expressed in the neurons of the neonatal and adult mammalian brains (Bouchier-Hayes, 2010; Carlsson et al., 2011; Di Donato et al., 2016) and is involved in apoptosis pathways, including DNA damage, mitochondria oxidative stress, and cytoskeletal disruption (Lassus et al., 2002; Bouchier-Hayes, 2010). After activation by PIDD1 and the formation of the PIDD1-RAIDD-caspase-2 complex, caspase-2 can trigger mitochondrial outer membrane permeability,

causing the release of cytochrome C from the mitochondria to the cytoplasm. Cytochrome C binds to apoptosis-related factor 1 (Apaf-1), promoting the formation of the apoptotic body by caspase-9, which activates caspase-3 and executes apoptosis. In the present study, after OGD, the levels of PIDD1, caspase-2, cytosolic cytochrome C, and cleaved caspase-3 were significantly increased compared with those in the control condition. When Neat1 was downregulated, the levels of PIDD1 and caspase-2 increased. In contrast, when Neat1 was upregulated, the levels of PIDD1 and caspase-2 decreased dramatically. Furthermore, the levels of downstream factors, including cytosolic cytochrome C and cleaved caspase-3, were also increased when Neat1 was downregulated and decreased when Neat1 was upregulated. These results indicated that the upregulation of Neat1 might reduce the levels of PIDD1, decreasing caspase-2-mediated apoptosis.

Mitochondrial dysfunction is thought to be involved in neuronal apoptosis, which plays an important role in many central nervous system diseases (Richter et al., 2015; Xie et al., 2018; Feng et al., 2020). Caspase-2 is thought to be the initiator that acts upstream of the mitochondria and permeabilizes the outer mitochondrial membrane, facilitating cytochrome C release (Lassus et al., 2002; Robertson et al., 2004; Clark et al., 2007). To further study the relationship between caspase-2 and cytochrome C in response to the down- and upregulation of Neat1 after OGD, the cytochrome C levels in the cytoplasm and mitochondria were measured. The results showed that after OGD, the level of cytosolic cytochrome C was highest, and the level of mitochondrial cytochrome C was lowest in neurons following Neat1 downregulation. The upregulation of Neat1 caused neurons to have significantly lower levels of cytosolic cytochrome C but significantly higher levels of mitochondrial cytochrome C compared with the effects of Neat1 downregulation. This suggested that upregulated Neat1 after OGD may significantly decrease the release of cytochrome C from mitochondria to the cytoplasm, indicating Neat1 may inhibit the neuronal apoptosis initiated by caspase-2 and mitochondrial dysfunction.

Neat1 plays a protective role during the injury process caused by OGD and might influence the viability and apoptosis of neurons after OGD. Furthermore, Neat1 may depress neuronal apoptosis by decreasing the levels of PIDD1 and caspase-2, subsequently reducing the release of cytochrome C from the mitochondria to the cytoplasm and reducing the level of caspase-3. However, the specific mechanism through which Neat1 acts on PIDD1 is not yet clear. In a future study, we will further explore the specific mechanisms through which Neat1 regulates PIDD1 and the interactions between PIDD1 and caspase-2, cleaved caspase-3, cytochrome C, and other proteins, to further illustrate the specific mechanism through which Neat1 regulates neuronal apoptosis.

Acknowledgments: Thanks for the experimental site and facilities provided by Ophthalmology Laboratory of the First Affiliated Hospital of Chongqing Medical University, China.

Author contributions: LJ and JJZ conceived and designed research; WNC, YFW and WT carried out experiments; ZMW analyzed data; QHS and YZ explained experimental results; WNC prepared pictures; WNC and LJ drafted manuscripts; XCS revised manuscripts; YFX and WD edited and revised manuscripts. All authors approved the final version of the paper.

Conflicts of interest: The authors declare that there are no conflicts of interest associated with this manuscript.

Financial support: This work was supported by the Youth Science Foundation Project of the National Natural Science Foundation of China, No. 81701226 (to LJ). The funding source had no role in study conception and design, data analysis or interpretation, paper writing or deciding to submit this paper for publication.

Institutional review board statement: All experimental procedures and protocols were approved by the Experimental Animal Ethics Committee of the First Affiliated Hospital of Chongqing Medical University of China on

December 19, 2020 (approval No. 2020-895). The experimental procedure followed the United States National Institutes of Health Guide for the Care and Use of Laboratory Animals (NIH Publication No. 85-23, revised 1996).

Copyright license agreement: The Copyright License Agreement has been signed by all authors before publication.

Data sharing statement: Datasets analyzed during the current study are available from the corresponding author on reasonable request.

Plagiarism check: Checked twice by iThenticate.

Peer review: Externally peer reviewed.

Open access statement: This is an open access journal, and articles are distributed under the terms of the Creative Commons Attribution-NonCommercial-ShareAlike 4.0 License, which allows others to remix, tweak, and build upon the work non-commercially, as long as appropriate credit is given and the new creations are licensed under the identical terms.

Open peer reviewers: Guilherme R. França, Universidade Federal Fluminense, Brazil; Jonathan M. Borkum, University of Maine, USA.

Additional file: Open peer review reports 1 and 2.

References

- Bewig B, Schmidt WE (2000) Accelerated titrating of adenoviruses. *Biotechniques* 28:870-873.
- Bock FJ, Peintner L, Tanzer M, Manzl C, Villunger A (2012) P53-induced protein with a death domain (PIDD): master of puppets? *Oncogene* 31:4733-4739.
- Bouchier-Hayes L (2010) The role of caspase-2 in stress-induced apoptosis. *J Cell Mol Med* 14:1212-1224.
- Carlsson Y, Schwendimann L, Vontell R, Rousset CI, Wang X, Lebon S, Charriat-Marlangue C, Supramaniam V, Hagberg H, Gressens P, Jacotot E (2011) Genetic inhibition of caspase-2 reduces hypoxic-ischemic and excitotoxic neonatal brain injury. *Ann Neurol* 70:781-789.
- Clark RS, Nathaniel PD, Zhang X, Dixon CE, Alber SM, Watkins SC, Melick JA, Kochanek PM, Graham SH (2007) boc-Aspartyl (OME)-fluoromethylketone attenuates mitochondrial release of cytochrome c and delays brain tissue loss after traumatic brain injury in rats. *J Cereb Blood Flow Metab* 27:316-326.
- Di Donato N, Jean YY, Maga AM, Krewson BD, Shupp AB, Avrutsky MI, Roy A, Collins S, Olds C, Willert RA, Czaja AM, Johnson R, Stover JA, Gottlieb S, Bartholdi D, Rauch A, Goldstein A, Boyd-Kyle V, Aldinger KA, Mirzaa GM, et al. (2016) Mutations in CRADD result in reduced caspase-2-mediated neuronal apoptosis and cause megalencephaly with a rare lissencephaly variant. *Am J Hum Genet* 99:1117-1129.
- Di Y, Wang Y, Wang X, Nie QZ (2021) Effects of long non-coding RNA myocardial infarction-associated transcript on retinal neovascularization in a newborn mouse model of oxygen-induced retinopathy. *Neural Regen Res* 16:1877-1881.
- Feng ST, Wang ZZ, Yuan YH, Wang XL, Sun HM, Chen NH, Zhang Y (2020) Dynamin-related protein 1: a protein critical for mitochondrial fission, mitophagy, and neuronal death in Parkinson's disease. *Pharmacol Res* 151:104553.
- Gong W, Zheng J, Liu X, Ma J, Liu Y, Xue Y (2016) Knockdown of NEAT1 restrained the malignant progression of glioma stem cells by activating microRNA let-7e. *Oncotarget* 7:62208-62223.
- Guo J, Cheng C, Chen CS, Xing X, Xu G, Feng J, Qin X (2016) Overexpression of fibulin-5 attenuates ischemia/reperfusion injury after middle cerebral artery occlusion in rats. *Mol Neurobiol* 53:3154-3167.
- Guru SC, Agarwal SK, Manickam P, Olufemi SE, Crabtree JS, Weisemann JM, Kester MB, Kim YS, Wang Y, Emmert-Buck MR, Liotta LA, Spiegel AM, Boguski MS, Roe BA, Collins FS, Marx SJ, Burns L, Chandrasekharappa SC (1997) A transcript map for the 2.8-Mb region containing the multiple endocrine neoplasia type 1 locus. *Genome Res* 7:725-735.
- Hackenberg K, Unterberg A (2016) Traumatic brain injury. *Nervenarzt* 87:203-214;quiz 215-216.
- Janssens S, Tinel A (2012) The PIDDosome, DNA-damage-induced apoptosis and beyond. *Cell Death Differ* 19:13-20.
- Jiang L, Zhong J, Dou X, Cheng C, Huang Z, Sun X (2015) Effects of ApoE on intracellular calcium levels and apoptosis of neurons after mechanical injury. *Neuroscience* 301:375-383.
- Kim IR, Murakami K, Chen NJ, Saibil SD, Matysiak-Zablocki E, Elford AR, Bonnard M, Benchimol S, Jurisicova A, Yeh WC, Ohashi PS (2009) DNA damage- and stress-induced apoptosis occurs independently of PIDD. *Apoptosis* 14:1039-1049.
- Lassus P, Opitz-Araya X, Lazebnik Y (2002) Requirement for caspase-2 in stress-induced apoptosis before mitochondrial permeabilization. *Science* 297:1352-1354.
- Marr RA, Hitt M, Muller WJ, Gaudie J, Graham FL (1998) Tumour therapy in mice using adenovirus vectors expressing human TNF α . *Int J Oncol* 12:509-515.
- Pei X, Li Y, Zhu L, Zhou Z (2019) Astrocyte-derived exosomes suppress autophagy and ameliorate neuronal damage in experimental ischemic stroke. *Exp Cell Res* 382:111474.
- Reng CM, Liu YF, Xu N, Shao MM, He JY, Li XJ (2020) Non-coding RNAs in human dental pulp stem cells: regulations and mechanisms. *Zhongguo Zuzhi Gongcheng Yanjiu* 24:1130-1137.
- Richter V, Singh AP, Kvensakul M, Ryan MT, Osellame LD (2015) Splitting up the powerhouse: structural insights into the mechanism of mitochondrial fission. *Cell Mol Life Sci* 72:3695-3707.
- Robertson JD, Gogvadze V, Kropotov A, Vakifahmetoglu H, Zhivotovskiy B, Orrenius S (2004) Processed caspase-2 can induce mitochondria-mediated apoptosis independently of its enzymatic activity. *EMBO Rep* 5:643-648.
- Salvador E, Burek M, Forster CY (2015) Stretch and/or oxygen glucose deprivation (OGD) in an in vitro traumatic brain injury (TBI) model induces calcium alteration and inflammatory cascade. *Front Cell Neurosci* 9:323.
- Sunwoo JS, Lee ST, Im W, Lee M, Byun JI, Jung KH, Park KI, Jung KY, Lee SK, Chu K, Kim M (2017) Altered expression of the long noncoding RNA NEAT1 in Huntington's disease. *Mol Neurobiol* 54:1577-1586.
- Tajiri N, Acosta SA, Shahaduzzaman M, Ishikawa H, Shinozuka K, Pabon M, Hernandez-Ontiveros D, Kim DW, Metcalf C, Staples M, Dailey T, Vasconcellos J, Franyuti G, Gould L, Patel N, Cooper D, Kaneko Y, Borlongan CV, Bickford PC (2014) Intravenous transplants of human adipose-derived stem cell protect the brain from traumatic brain injury-induced neurodegeneration and motor and cognitive impairments: cell graft biodistribution and soluble factors in young and aged rats. *J Neurosci* 34:313-326.
- Tang YL, Fang LJ, Zhong LY, Jiang J, Dong XY, Feng Z (2020) Hub genes and key pathways of traumatic brain injury: bioinformatics analysis and in vivo validation. *Neural Regen Res* 15:2262-2269.
- Wang X, Tong J, Han X, Qi X, Zhang J, Wu E, Huang JH (2020) Acute effects of human protein S administration after traumatic brain injury in mice. *Neural Regen Res* 15:2073-2081.
- Wong N, Blair AR, Morahan G, Andrikopoulos S (2010) The deletion variant of nicotinamide nucleotide transhydrogenase (Nnt) does not affect insulin secretion or glucose tolerance. *Endocrinology* 151:96-102.
- Xie LL, Shi F, Tan Z, Li Y, Bode AM, Cao Y (2018) Mitochondrial network structure homeostasis and cell death. *Cancer Sci* 109:3686-3694.
- Yang C, Li Z, Li Y, Xu R, Wang Y, Tian Y, Chen W (2017) Long noncoding RNA NEAT1 overexpression is associated with poor prognosis in cancer patients: a systematic review and meta-analysis. *Oncotarget* 8:2672-2680.
- Yang L, Cui H, Cao T (2014) Negative regulation of miRNA-9 on oligodendrocyte lineage gene 1 during hypoxic-ischemic brain damage. *Neural Regen Res* 9:513-518.
- Zanelli SA, Rajasekaran K, Grosenbaugh DK, Kapur J (2015) Increased excitability and excitatory synaptic transmission during in vitro ischemia in the neonatal mouse hippocampus. *Neuroscience* 310:279-289.
- Zhang Q, Cheng Q, Xia M, Huang X, He X, Liao J (2020) Hypoxia-induced lncRNA-NEAT1 sustains the growth of hepatocellular carcinoma via regulation of miR-199a-3p/UCK2. *Front Oncol* 10:998.
- Zhen L, Yun-Hui L, Hong-Yu D, Jun M, Yi-Long Y (2016) Long noncoding RNA NEAT1 promotes glioma pathogenesis by regulating miR-449b-5p/c-Met axis. *Tumour Biol* 37:673-683.
- Zhong J, Jiang L, Cheng C, Huang Z, Zhang H, Liu H, He J, Cao F, Peng J, Jiang Y, Sun X (2016) Altered expression of long non-coding RNA and mRNA in mouse cortex after traumatic brain injury. *Brain Res* 1646:589-600.
- Zhong J, Jiang L, Huang Z, Zhang H, Cheng C, Liu H, He J, Wu J, Darwazeh R, Wu Y, Sun X (2017) The long noncoding RNA Neat1 is an important mediator of the therapeutic effect of bexarotene on traumatic brain injury in mice. *Brain Behav Immun* 65:183-194.

P-Reviewers: França GR, Borkum JM; *C-Editor:* Zhao M; *S-Editors:* Wang J, Li CH; *L-Editors:* Qiu Y, Song LP; *T-Editor:* Jia Y